The Holocene

Holocene changes in atmospheric circulation recorded in the oxygen-isotope stratigraphy of lacustrine carbonates from northern Sweden

Dan Hammarlund, Lena Barnekow, H. J.B. Birks, Bjørn Buchardt and Thomas W.D. Edwards

The online version of this article can be found at:

Published by:

SSAGE Publications

Additional services and information for *The Holocene* can be found at:

Email Alerts: http://hol.sagepub.com/cgi/alerts

Subscriptions: http://hol.sagepub.com/subscriptions

Reprints: http://www.sagepub.com/journalsReprints.nav

Permissions: http://www.sagepub.com/journalsPermissions.nav

Citations (this article cites 45 articles hosted on the
SAGE Journals Online and HighWire Press platforms):
http://hol.sagepub.com/cgi/content/refs/12/3/339

Holocene changes in atmospheric circulation recorded in the oxygen-isotope stratigraphy of lacustrine carbonates from northern Sweden

Dan Hammarlund,[1]* Lena Barnekow,[1] H.J.B. Birks,[2]
Bjørn Buchardt[3] and Thomas W.D. Edwards[4]

(*[1]Department of Quaternary Geology, Lund University, Tornav. 13, SE-223 63 Lund, Sweden; [2]Botanical Institute, University of Bergen, Allég. 41, N-5007 Bergen, Norway, and Environmental Change Research Centre, University College London, 26 Bedford Way, London, WC1H 0AP, UK; [3]Geological Institute, University of Copenhagen, Øster Voldg. 10, DK-1350 Copenhagen K, Denmark; [4]Department of Earth Sciences and Quaternary Sciences Institute, University of Waterloo, Waterloo, ON N2L 3G1, Canada)*
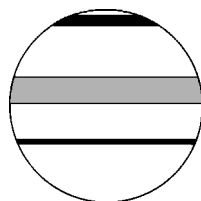
Abstract: The oxygen-isotope composition of local precipitation ($\delta^{18}O_P$) is reconstructed from carbonate lake-sediment components in a sediment core covering the last 10000 calendar years from Lake Tibetanus, a small, hydrologically open, groundwater-fed lake in the Abisko area, northern Sweden. Comparison of the $\delta^{18}O_P$ history with a pollen-based palaeotemperature record from the same core clearly reveals pronounced deviations from the normally expected temporal $\delta^{18}O_P$-temperature relation (so-called 'Dansgaard relation') that may be a function of changing oceanicity. The transition from relatively moist, maritime conditions in the early Holocene to a much drier climate after 6500 cal. BP is reflected by major changes in forest extent and composition as recorded by pollen and plant macrofossil data. At the time of maximum influence of westerly air-mass circulation (high zonal index) *c*. 9500 cal. BP, brought about by high summer insolation and enhanced meridional pressure gradients, $\delta^{18}O_P$ at Lake Tibetanus was about 2‰ higher than would be predicted by the modern isotope-temperature relation. The occurrence of long-term changes in $\delta^{18}O_P$-temperature relations, which are more sensitive measures of palaeoclimate than either $\delta^{18}O_P$ or temperature alone, needs to be taken into account when extracting palaeoclimatic information from continental oxygen-isotope records.

Key words: Palaeoclimate, atmospheric circulation, stable isotopes, oxygen-isotope stratigraphy, lacustrine carbonates, pollen-climate transfer functions, Holocene, northern Sweden.

Introduction

Coupling of isotopic, geochemical and palaeoecological analyses of different components in lacustrine deposits can be an effective strategy for obtaining information about past climatic and environmental changes (e.g., MacDonald *et al.*, 1993; Hammarlund and Lemdahl, 1994; Schwalb *et al.*, 1995). The use of water-isotope tracers (most commonly ^{18}O) in continental palaeoenvironmental studies is especially promising because of the potential links to past synoptic isotope climatology and hydrology (e.g., Amundson

et al., 1996; Edwards *et al.*, 1996; Wolfe *et al.*, 2000). These can be represented with increasing precision by atmospheric general circulation models incorporating water-isotope tracer diagnostics (Joussaume and Jouzel, 1993; Jouzel *et al.*, 1996; Hoffmann *et al.*, 2000). Although commonly reflecting palaeotemperature at the site of condensation (Dansgaard, 1964), the isotopic composition of palaeoprecipitation is being increasingly utilized as a source of evidence for changes in parameters such as moisture source, air-mass trajectories and rain-out history, and seasonality (e.g., Plummer, 1993; McKenzie and Hollander, 1993; Charles *et al.*, 1994; Edwards *et al.*, 1996; Stute and Talma, 1998).

Here we focus on the quantitative characterization of past

*Author for correspondence (e-mail: dan.hammarlund@geol.lu.se)

isotope-climate relations in the Abisko area, northernmost Sweden, based on independent reconstructions of the oxygen-isotope composition of local palaeoprecipitation and local palaeotemperature, both derived from the Holocene sediment sequence of Lake Tibetanus, a small hard-water lake close to the present-day altitudinal tree-line on the eastern flank of the Scandes Mountains. This study is part of an ongoing effort to reconstruct Holocene climatic and vegetational changes in the Abisko area using multi-proxy methods (see Berglund *et al.*, 1996).

The Scandes Mountains, the main north–south mountain range in Sweden and Norway, exhibit a wide variety of climatic and hence phytogeographical regimes today. Proximity to the North Atlantic with its prevailing influence of oceanic air-masses, as well as to the polar atmospheric front, makes the area particularly suitable for studies of ecoclimatic gradients. Although stable and well-defined ecological gradients and topographical vegetation zonations aligned west–east and north–south occur in the mountain chain at present (Sjörs, 1963), palaeoecological and geological evidence suggest that substantial changes in the climatic parameters responsible for these patterns have occurred during the Holocene (e.g., Kullman, 1988; 1992; 1993; 1995; 1999; Karlén and Kuylenstierna, 1996; Dahl and Nesje, 1996; Barnekow, 1999; 2000; Matthews *et al.*, 2000).

Prior studies of particular relevance to the present paper include consideration of carbon-isotope records from Lake Tibetanus in the context of local soil maturation and aquatic carbon cycling (Hammarlund *et al.*, 1997), detailed interpretation of the local Holocene terrestrial vegetation history based on pollen and plant macrofossil analyses (Barnekow, 1999), and the development and validation of robust pollen-based climate transfer functions from modern calibration studies in the region. The last two efforts are particularly crucial for the present discussion, which substantiates previous speculation that changes in the distillation of moisture transported across the Scandes Mountains, in response to changing atmospheric zonal index, made an important imprint on the isotopic composition of palaeoprecipitation in the Abisko area during the early to mid-Holocene (Berglund *et al.*, 1996; Hammarlund and Edwards, 1998). Insight gained from consideration of modern isotope hydrological data also helps to place firmer constraints on the isotope palaeohydrology of Lake Tibetanus.

Site description

Lakes in the Abisko area were described by Ekman (1957), and the setting and characteristics of Lake Tibetanus were presented by Berglund *et al.* (1996) and Hammarlund *et al.* (1997). Briefly, it is situated in the upper mountain-birch zone at *c.* 560 m a.s.l. on glacial and colluvial deposits mantling the lower part of the south-facing slope of Mount Slåttatjåkka (1191 m) within the Abisko National Park in the northern part of the Scandes Mountains (68°20′N, 18°42′E; Figure 1). The basin is 85–100 m in diameter and has a maximum depth of 3.9 m. The lake primarily receives inflow from groundwater springs at the upslope (northern) margin. In addition to downslope seepage, surface outflow occurs via a well-defined channel passing through a wetland on the southeast. Existence of a stable hard-water effect through time, based on radiocarbon dating of terrestrial macrofossils and other sediment constituents, as well as consistent $\delta^{13}C$ offsets between the three carbonate components analysed (Figure 2; Hammarlund *et al.*, 1997) demonstrate that Lake Tibetanus has been characterized by consistently rapid flushing rates throughout its existence. Indeed, although Hammarlund *et al.* (1997) conservatively assumed a residence time of two to four months under present conditions, reconsideration of the physical setting, lake volume and discharge, and the absence of detectable evaporative isotopic enrichment of the
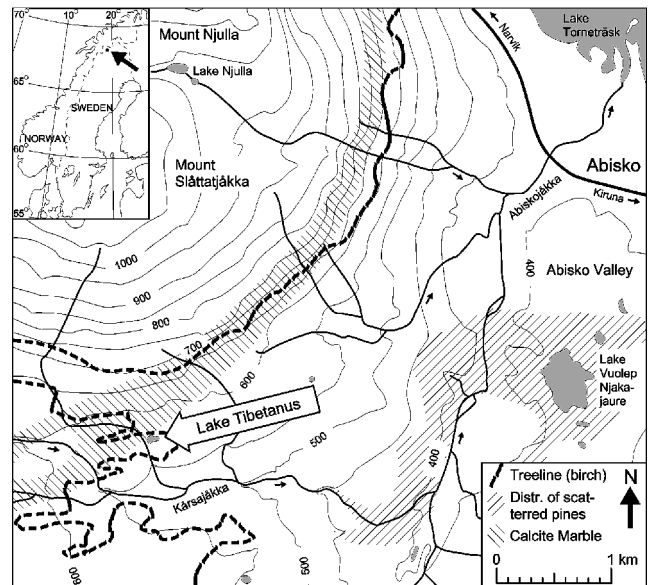

Figure 1 Map of the study area located in the northern part of the Scandes Mountains, northern Sweden (bold arrow on inset map).
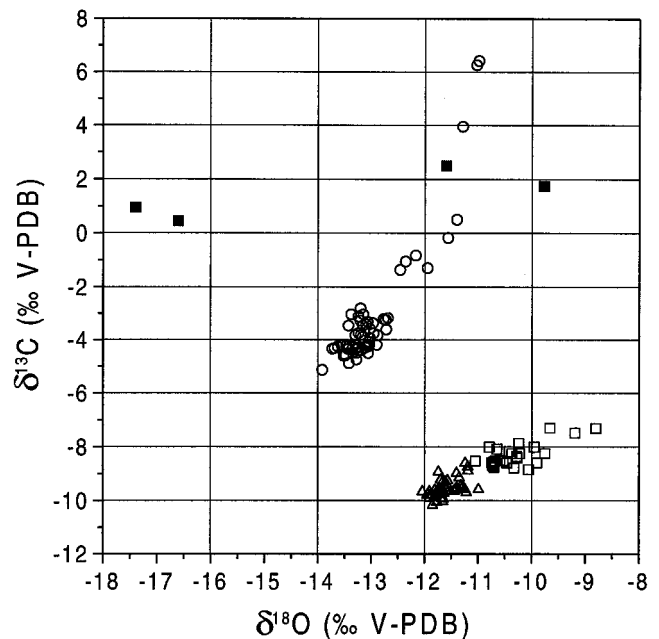

Figure 2 Carbon-isotope data from Lake Tibetanus plotted against corresponding oxygen-isotope data. Circles = fine-grained sedimentary carbonate (primarily *Chara* calcite). Triangles = *Pisidium* sp. mollusc aragonite. Open squares = adult *Candona candida* ostracode calcite. Solid squares indicate isotopic data obtained on samples of the local calcite marble. See Hammarlund *et al.* (1997) for further details and interpretation of the carbon-isotope records.

lakewater (see below) suggest that the residence time is probably no more than a few weeks.

Dissolved inorganic carbon is supplied in abundance from dissolution of the calcareous overburden and local calcite marble bedrock, which outcrops upslope of the lake (Figure 1; Kulling, 1964), leading to the production and preservation of carbonate-rich sediments, as well as high lakewater electrical conductivity and pH (Table 1). The aquatic vegetation is sparse and composed mainly of charophytes (*Chara* spp.), typical for mid- to high-latitude hard-water lakes. The terrestrial vegetation of the catchment is dominated by heath communities with dwarf birch (*Betula nana* L.), dwarf shrubs (Ericales) and willows (*Salix* spp.), intermixed with open stands of mountain birch (*Betula pubescens*

Table 1 Measured or estimated physical and chemical parameters of Lake Tibetanus. Water-temperature data were reported by Ekman (1957)

Measured/estimated parameter	Result
Lake area	*c.* 4600 m^2
Maximum water depth	3.9 m
Mean water depth (estimated)	*c.* 2 m
Lake volume	*c.* 9000 m^3
Catchment area (estimated)	*c.* 250000 m^2
Outflow discharge (estimated)	*c.* 51 s^{-1} = *c.* 160000 m^3 yr^{-1}
Residence time	20–25 days
July water temperature	6.8–8.5°C
August water temperature	8.5–11.4°C
Approximate period of ice cover	mid-October to early June
pH (under ice in March 1996)	7.7
Conductivity (March 1996)	622 µS at 0°C

Ehrh. ssp. *tortuosa* (Ledeb.) Nyman), especially on the northern side of the lake. Scattered groups of Scots pine (*Pinus sylvestris* L.) occur on south-facing, well-drained hillslopes below *c.* 450 m a.s.l. within the subalpine birch forest of the adjacent Abisko valley. The Abisko area lies in the rain shadow of the Scandes Mountains, which act as a barrier to atmospheric moisture carried by westerly winds, as shown by the strong precipitation gradient that is evident from climatic data compiled for a series of meteorological stations on a west–east transect across the study area (Table 2). In spite of the low mean annual precipitation at Abisko (*c.* 300 mm), net precipitation (P-E) is relatively high due to low rates of evapotranspiration (Ovhed and Holmgren, 1996).

Methods

Fieldwork and subsampling

Multiple core drives at staggered stratigraphical intervals were retrieved from the deepest, western part of the lake in March 1995 at a water depth of 3.9 m, using 6.5 and 10 cm diameter, 1 m long Russian peat samplers, working from the ice surface. The entire sediment sequence was extruded and described in the field prior to shipment to the laboratory, where the core increments were correlated and subdivided into 61 contiguous sections, 20–68 mm thick, allowing for lithostratigraphical boundaries. Small subsamples were separated for elemental carbon and stable-isotope analyses, and the remaining parts of the main sections were further divided into two or three subsamples, 17–26 mm thick, for radiocarbon dating and macrofossil analysis

(Hammarlund *et al.*, 1997; Barnekow *et al.*, 1998; Barnekow, 1999).

Stable-isotope analyses

Oxygen-isotope analysis of fine-grained sedimentary calcite was undertaken on aliquots of freeze-dried sediment that had been gently passed through a 125 µm sieve to eliminate fragments of mollusc shells and ostracode valves. The sedimentary calcite δ^{18}O record was complemented by a surface-sediment sample obtained from a gravity core collected in July 1995. Shells and valves for separate isotopic analysis were picked by hand from the >250 µm sediment fraction after wet-sieving. Carbonate samples (*c.* 5 mg fine-grained sedimentary calcite, 2–12 single shells of *Pisidium* sp. bivalves, or 4–20 single valves of *Candona candida* ostracodes) were dissolved in phosphoric acid and the ^{18}O/^{16}O ratio was determined on the evolved carbon dioxide by mass spectrometry at the University of Copenhagen (sedimentary calcite and *Pisidium* sp.) and the University of Bergen (*C. candida*), using standard methods (McCrea, 1950; Buchardt, 1977). The results are expressed as δ^{18}O values, representing deviations in per mil (‰) from the V-PDB standard, such that δ^{18}O$_{sample}$ = [(R_{sample}/$R_{standard}$) − 1] × 1000‰, where R is the ^{18}O/^{16}O ratio in sample and standard. Analytical uncertainties are within ±0.07‰.

Water samples collected from the lake and its vicinity during the period 1995–98 (Table 3) were analysed for stable oxygen- and hydrogen-isotope compositions at the University of Waterloo and the University of Copenhagen using the conventional CO$_2$-equilibration and Zn-reduction methods, respectively (Epstein and Mayeda, 1953; Coleman *et al.*, 1982). The results are expressed in the δ notation (see above) relative to V-SMOW (Vienna-Standard Mean Ocean Water), normalized so that the respective δ^{18}O and δ^{2}H values of SLAP (Standard Light Antarctic Precipitation) are –55.5‰ and –428‰ relative to V-SMOW, as recommended by Coplen (1996). Analytical uncertainties are within ±0.2‰ and ±2‰ for δ^{18}O and δ^{2}H, respectively.

Vegetational analyses and pollen-based climate reconstructions

Pollen and plant macrofossil analysis methods were described in detail by Barnekow (1999). The pollen record presented by Barnekow (1999) was used for quantitative reconstructions of mean July temperature and mean annual precipitation employing a modern pollen-climate calibration set of 191 surface samples from lakes throughout Norway and northern Sweden (Seppä and Birks, 2001). All samples were taken from the deepest part of small (100–300 m diameter) lakes using a gravity corer (Renberg, 1991), with the uppermost 1 cm of sediment retained as the surface sample. Lakes were avoided that had extensive marginal

Table 2 Meteorological data from four monitoring stations along a west–east transect through the study site (Alexandersson *et al.*, 1991; Josefsson, 1990). Temperature data for Lake Tibetanus have been extrapolated from values compiled by Josefsson (1990) for different altitudes in the Abisko valley during the period 1951–80

	Riksgränsen	Katterjåkk	Lake Tibetanus	Abisko	Torneträsk
Altitude	508 m a.s.l.	500 m a.s.l.	560 m a.s.l.	388 m a.s.l.	393 m a.s.l.
Location	68°25′N, 18°08′E	68°25′N, 18°10′E	68°20′N, 18°42′E	68°21′N, 18°49′E	68°13′N, 19°43′E
Distance from Lake Tibetanus	26 km (WNW)	24 km (WNW)	–	6 km (ENE)	44 km (ESE)
Mean annual air temperature	–1.4°C	–1.7°C	*c.* –1.4°C	–1.0°C/–0.8°C	–1.0°C
Mean January air temperature	–11.4°C	–11.9°C	*c.* –11.0°C	–11.7°C/–11.9°C	–12.7°C
Mean July air temperature	+10.1°C	+10.5°C	*c.* +10.4°C	+11.3°C/+11.0°C	+11.8°C
Monitoring period (temp.)	1961–72	1972–90	1951–80 (extr.)	1951–80/1961–90	1971–90
Mean annual precipitation	1001 mm	848 mm	no data	322 mm/304 mm	472 mm
Ratio of snow to total precip.	no data	no data	no data	*c.* 50%	no data
Monitoring period (precip.)	1961–73	1969–90	no data	1951–80/1961–90	1971–90
Mean annual evaporation	*c.* 100 mm	*c.* 100 mm	100–150 mm	100–150 mm	100–150 mm

Table 3 Isotopic data from water samples collected in the catchment of Lake Tibetanus (560 m a.s.l.) and surrounding areas (Figure 1)

Site	Date	$\delta^{18}O$	δ^2H
Inflow (groundwater spring)	3 July 1995	−14.96	−107.3
Inflow (groundwater spring)	29 June 1997	−14.76	−102.5
Inflow (groundwater spring)	18 March 1998	−15.65	−106.5
Inflow (groundwater spring)	7 October 1998	−14.34	−101.6
Lake surface	3 July 1995	−14.42	−106.0
Lake surface	5 July 1995	−14.47	−107.9
Lake under ice	11 March 1996	−15.03	−107.0
Lake surface	19 March 1997	−13.97	−98.8
Lake surface	29 June 1997	−14.36	−102.1
Lake at 2.5 m depth	29 June 1997	−14.48	−101.5
Lake surface	5 September 1997	−13.51	−96.2
Lake under ice	16 March 1998	−14.95	−105.4
Lake surface	7 October 1998	−14.20	−100.1
Snow patch near the lake	3 July 1995	−14.01	−97.1
Snow on the lake ice	12 March 1996	−13.55	−93.8
Snow on the lake ice	19 March 1997	−12.38	−69.1
Snow patch near the lake	29 June 1997	−15.51	−110.1
Snow on the lake ice	16 March 1998	−11.80	−81.5
Snow patch at *c.* 1000 m a.s.l.	29 June 1997	−13.54	−90.8
Snow patch at *c.* 1000 m a.s.l.	5 September 1997	−11.25	−74.0
Snow at *c.* 1000 m a.s.l.	14 March 1998	−21.36	−149.8
Snow at *c.* 700 m a.s.l.	7 October 1998	−8.39	−43.7
Snow at *c.* 900 m a.s.l.	7 October 1998	−9.05	−50.4
Snow at *c.* 1000 m a.s.l.	7 October 1998	−8.81	−48.2
Snow at Abisko (388 m a.s.l.)	12 March 1996	−16.70	−112.7
Snow at Abisko (388 m a.s.l.)	21 March 1997	−28.52	−211.0
Snow at Abisko (388 m a.s.l.)	10 September 1997	−17.84	−116.9
Snow at Abisko (388 m a.s.l.)	13 March 1998	−21.68	−156.5
Rain at Abisko (388 m a.s.l.)	10 July 1995	−12.72	−98.2
Rain at Abisko (388 m a.s.l.)	29 June 1997	−6.63	−58.1
Rain at Abisko (388 m a.s.l.)	3 October 1998	−15.40	−123.8
Rain at Abisko (388 m a.s.l.)	4 October 1998	−7.68	−46.8

Isotopic units: ‰ (V-SMOW)

sedge-swamps or intensive land use or other disturbances within their catchments. Because the pollen-morphological resolution is different between the modern data set and the Lake Tibetanus pollen-stratigraphical record, the data sets were harmonized to the lowest possible consistent taxonomic level.

Modern mean July temperatures and mean annual precipitation values were estimated for each of the 191 lakes using the 1961–90 climate reference-normals data from grids of nearby meteorological stations in Norway and Sweden. Mean annual precipitation figures were estimated by interpolation between climate stations with allowance for elevation. Mean July temperatures were derived by applying a lapse rate of 0.57°C per 100 m altitude (Laaksonen, 1976) to allow for temperature changes along elevational gradients and by applying empirically derived regional west–east lapse rates to allow for temperature changes with distance from the coast for lakes west of the Scandes Mountains.

Modern pollen-climate transfer functions were developed using weighted-averaging partial least squares (WA-PLS) regression (ter Braak and Juggins, 1993; Birks, 1995). All harmonized terrestrial pollen and spore taxa in the modern data set were used in the transfer function. Pollen percentages were transferred to square roots in an attempt to optimize the signal-to-noise ratio and to stabilize the variances. WA-PLS was selected because it has been shown in several empirical and theoretical studies to perform as well as, or even better than, other regression procedures used to develop organism-environment transfer functions (ter Braak *et al.*, 1993; ter Braak, 1995; Birks, 1995; 1998).

Table 4 Performance statistics for weighted-averaging partial least squares (WA-PLS) regression models for the modern pollen-climate data set (191 samples × 143 taxa) from Norway and northern Sweden. Root mean square error of prediction (RMSEP), coefficient of determination (r^2) and maximum bias are given based on leave-one-out cross-validation for 1, 2 and 3 component WA-PLS models for mean July temperature and mean annual precipitation. The models used for reconstruction are shown in bold, following the criteria of model selection of ter Braak and Juggins (1993) and Birks (1998)

Components	RMSEP	r^2	Maximum bias
Mean July temperature (°C)			
1	1.07	0.50	3.97
2	**1.05**	**0.53**	**3.71**
3	1.04	0.54	3.54
Annual precipitation (mm)			
1	426.57	0.66	1121.69
2	**418.24**	**0.68**	**957.03**
3	437.64	0.65	928.71

The performance of the WA-PLS transfer functions is reported here (Table 4) as the root mean square error of prediction (RMSEP), the coefficient of determination (r^2), and the maximum bias (ter Braak and Juggins, 1993), all based on leave-one-out cross-validation (ter Braak and Juggins, 1993; Birks, 1995). Two-component WA-PLS models were selected (Table 4) on the basis of low RMSEP, low maximum bias and the smallest number of 'useful' components (Birks, 1998). Plots of the residuals (predicted values in leave-one-out cross-validation – observed values) against observed values (not presented here) show that the transfer function estimates July temperature well above 10°C but that it overestimates July values below 10°C, presumably because far-blown pollen from the lowlands is often incorporated into surface sediments of lakes above the tree-line where cooler conditions prevail. There is no strong bias in the mean annual precipitation model, except for a tendency to underestimate mean annual precipitation at sites receiving more than 2000 mm precipitation. Full details of the modern pollen-climate data set will be published elsewhere.

Several reconstruction diagnostic statistics (Birks, 1995; 1998) were calculated to evaluate the potential reliability of the pollen-inferred reconstructions of mean July temperature and mean annual precipitation at Lake Tibetanus. These are: (1) analogue measures such as squared chord distance to identify if any fossil assemblages lack 'good' modern analogues within the modern calibration data set (Birks *et al.*, 1990); (2) the percentage of the fossil assemblages consisting of pollen and spore taxa absent from the modern calibration data set (Birks, 1998); (3) goodness-of-fit measures derived from a canonical correspondence analysis (CCA) (ter Braak and Šmilauer, 1998) of modern and fossil pollen spectra with the environmental variable of interest (e.g., July temperature) as the sole constraining variable to assess the statistical fit of the fossil assemblage to the environmental variable of interest (Birks *et al.*, 1990). We used the squared residual distance of the modern and fossil samples as a criterion of fit. Fossil spectra with a low squared residual distance from the environmentally constrained axis have a 'good' fit to that environmental variable. Any fossil sample with a squared residual distance equal to, or greater than, the squared residual distance of the extreme 10% of the modern calibration samples is considered to have a 'poor' fit to that environmental variable (Birks *et al.*, 1990).

Sediment description and chronology

The 2.95 m thick sequence was classified into six lithostratigraphical units partly based on carbon content (Table 5). The lowermost 0.15 m consists of carbonate-rich silt and sand, gradually changing into *c.* 0.8 m of pure, whitish lake marl (Figure 3). The lake marl is followed by *c.* 0.7 m of calcareous gyttja with abundant bark fragments and needles of pine and other macroscopic plant remains. The upper 1.3 m section consists of brownish to yellowish, laminated calcareous gyttja. Mollusc shells are plentiful above *c.* 2.5 m depth, but the sediments below this point are essentially devoid of mollusc shells or ostracode valves. X-ray diffraction analysis revealed that the <125 µm carbonate fraction of the sediments is exclusively low-Mg calcite. Strong enrichment in ^{13}C of bulk carbonates and the preservation of abundant millimetre-sized, tubular cryptocrystalline calcite encrustations formed on the stems of *Chara*, especially in the lower units of the sequence (Hammarlund *et al.*, 1997), suggest that the fine-grained sedimentary calcite was precipitated as a consequence of photosynthesis during the thaw season, and hence should be a good oxygen-isotope archive for palaeoenvironmental investigations. As shown in Figure 3, the chronology is based on the age-depth model of Barnekow *et al.* (1998), which is based on 11 AMS radiocarbon dates obtained from well-identified terrestrial macrofossils. The calendar-year age scale shown in Figure 4 is slightly modified in the older part of the sequence as compared to Barnekow (1999), following recalibration of the two lowermost radiocarbon dates according to the IntCal98 calibration data set (Stuiver *et al.*, 1998).

Vegetational history and pollen-based climate reconstruction

A detailed reconstruction of the Holocene vegetational history of the Abisko area has been presented previously (Barnekow, 1999), and these results were evaluated in a more regional framework by Barnekow (2000). Briefly, the pollen and plant macrofossil records from the Lake Tibetanus core indicate that mountain birch rapidly colonized the catchment of the lake after the local deglaciation at *c.* 10000 cal. BP. The following 3000–4000 year period

was characterized by a progressive succession from an open subarctic tundra with abundant herbs and dwarf shrubs, through subarctic and subalpine birch woodlands with grasses, sedges and ferns, to boreal pine-birch forest (Figure 4). This development, in harmony with other records from the region (Sonesson, 1974; Berglund *et al.*, 1996; Bigler *et al.*, 2002; Birks *et al.*, unpublished data), suggests a long-term change from relatively moist, oceanic conditions towards a more continental climate. An important feature is the marked early-Holocene extension in the elevational limit of mountain birch (*Betula pubescens*), which reached 300–400 m above the present tree-line by *c.* 9000 cal. BP (Barnekow, 1999), suggesting that the mean growing-season temperature was at least 1.5°C above that of the present.

Pine was an important forest component in the Abisko valley during the mid-Holocene, with its upper limit rising progressively to at least 175 m above the present-day limit (*c.* 450 m a.s.l.), reaching Lake Tibetanus at *c.* 6300 cal. BP. Pine-birch forest occupied the catchment of the lake until *c.* 3700 cal. BP as part of a major altitudinal expansion of this vegetation type. Pine disappeared from the Lake Tibetanus catchment around 3400 cal. BP, suggesting a regional retraction of its upper limit and decreased importance of pine in the evolving subalpine birch woodland, ultimately leading to the restricted modern distribution of pine in the Abisko area (Figure 1). The elevational retraction of the pine limit during the later part of the Holocene was accompanied by a general lowering of tree-line, which was composed of mountain birch. However, the presence of mountain birch megafossils at *c.* 1000 m a.s.l. until *c.* 5100 cal. BP (Kullman, 1999) suggests that growing-season temperatures at this stage might have exceeded present-day values by nearly 2°C (Barnekow, 2000), and a corresponding value of *c.* 1.5°C at *c.* 4500 cal. BP is inferred from the presence of pine at a site *c.* 65 m above Lake Tibetanus (Barnekow, 1999). Thus, a subsequent cooling must have taken place and the period after *c.* 3000 cal. BP was marked by a general decrease in birch-forest density, expansion of heath communities and increased soil erosion (Jonasson, 1991; Snowball, 1995; Berglund *et al.*, 1996; Barnekow, 1999), all suggestive of cooler summers and reduced seasonality.

Before considering the quantitative reconstructions of mean July temperature and mean annual precipitation based on applying modern pollen-climate transfer functions to the pollen stratigraphical record (Table 4), it is important to evaluate the reconstructions from a statistical and palaeoecological point of view (Birks *et al.*, 1990; Birks, 1995; 1998). Five of the pollen and spore taxa recorded in the Lake Tibetanus pollen stratigraphy are absent from the modern calibration data set. These taxa only account for 0.09–1.5% of the fossil assemblages and the statistical effect of their absence from the modern calibration data set is thus negligible. Of the 45 fossil pollen spectra at Lake Tibetanus, all but five have good modern analogues in the calibration pollen data set (Figure 4) with squared chord distances of 0.142 or less (extreme 10% percentile of modern distances). Four samples in the lower part of the pollen record have squared chord distances of 0.154–0.180, suggesting that they are not strongly different in their pollen composition from the modern data. The basal sample has a high squared chord distance (0.310) and thus has poor analogues in the modern calibration data set. As derived from CCA with mean July temperature and mean annual precipitation as the sole constraining predictor environmental variables, the squared residual distances of the fossil pollen spectra are generally low and do not fall within the extreme 10% of the modern squared residual distances, except for three of the samples indicated in Figure 4. These evaluations suggest that nearly all the reconstructed values of mean July temperature and mean annual precipitation are reliable statistically and palaeoecologically in that the fossil pollen spectra have good modern analogues within the

Table 5 Lithostratigraphic description of the sediment core (OC and CC represent organic and carbonate carbon contents respectively)

| Unit	Depth (m)	Description	OC (%)	CC (%)
5	0.0–0.06	Dark greenish grey, laminated calcareous gyttja	18.4	2.89
4b	0.06–1.33	Greyish brown/yellowish brown, distinctly laminated calcareous gyttja with occasional macroscopic plant remains	7.18–18.9	3.72–9.32
4a	1.33–2.01	Dark brown/greyish or yellowish brown, laminated calcareous gyttja with abundant macroscopic plant remains, gradually decreasing towards upper boundary	5.54–20.7	4.40–10.1
3	2.01–2.71	Yellowish white, faintly laminated lake marl	1.20–2.25	10.8–11.5
2	2.71–2.78	Grey/yellowish grey lake marl	1.36–1.41	11.3–11.4
1	2.78–2.95	Dark grey carbonate-rich silt with sand layers	0.579–1.78	2.36–10.4
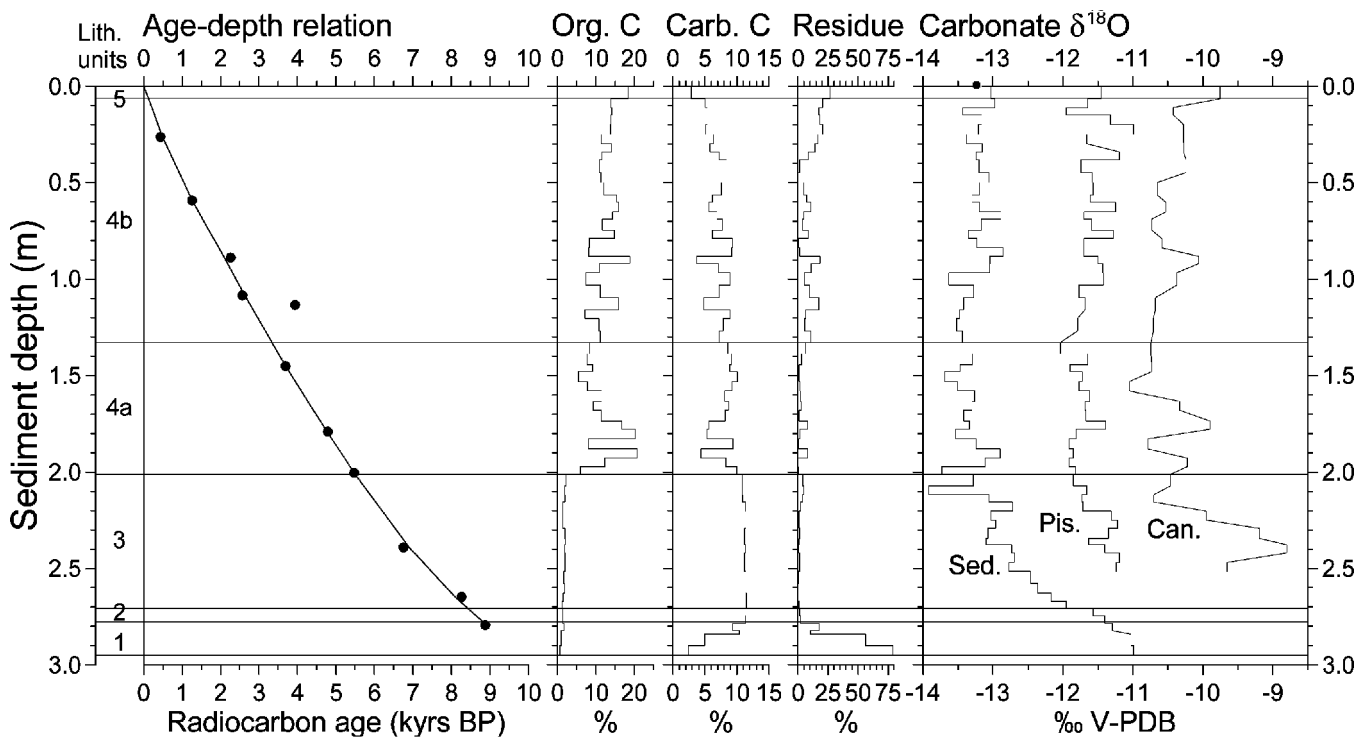
Figure 3 Age-depth model based on radiocarbon dates of terrestrial macrofossils (Barnekow *et al.*, 1998) together with lithological properties and oxygen-isotope records (Table 6) plotted against sediment depth. Carbon contents of the sediments are expressed as dry weight percentages of organic and carbonate elemental carbon (Org. C and Carb. C, respectively). Residue refers to an estimation of minerogenic content (non-carbon containing material) of the sediments based on the following calculation: residue = 100 − (OC*30/12) − (CC*100/12) (%). The molar weights of organic material and carbonates have been assigned values of 30 and 100 on the assumption of chemical compositions of CH_2O and $CaCO_3$ respectively. Sed. = fine-grained sedimentary carbonate (primarily *Chara* calcite); Pis. = *Pisidium* sp. mollusc aragonite; Can. = adult *Candona candida* ostracode calcite. The filled circle at 0.0 m represents modern $\delta^{18}O_{Sed}$ as determined on surface sediments. The left-hand column refers to the lithostratigraphic units as described in Table 5.
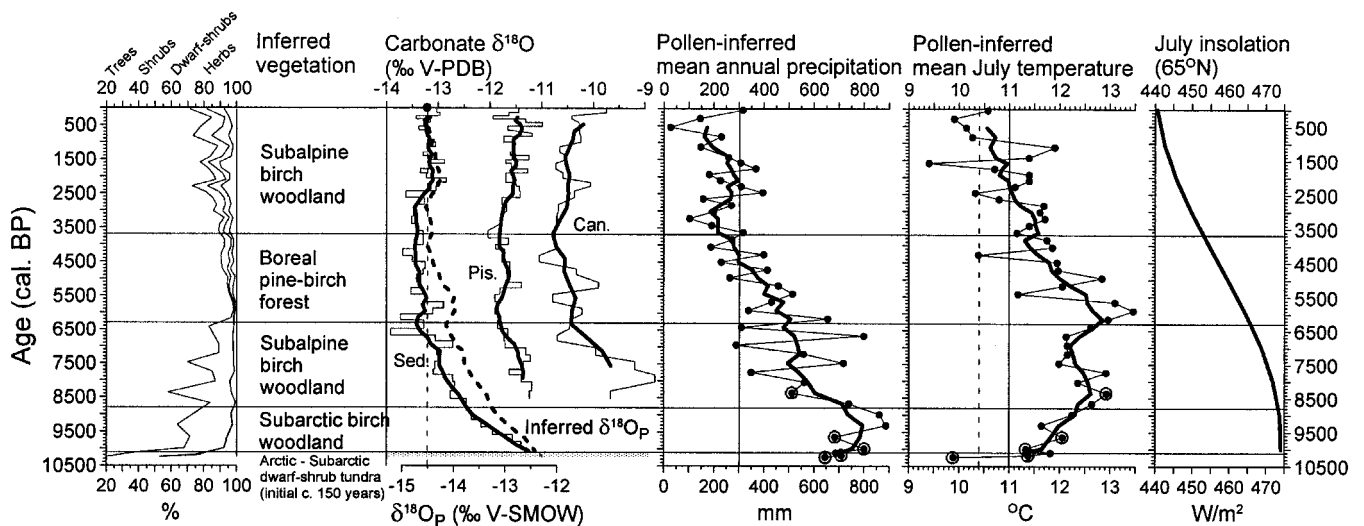

Figure 4 Oxygen-isotope records plotted against calibrated radiocarbon age (Stuiver *et al.*, 1998), along with a summary pollen-percentage diagram from the same core, a zonation of the local vegetational development based on pollen and macrofossil data (Barnekow, 1999), and pollen-inferred reconstructions of mean July temperature and mean annual precipitation. Samples with poor modern pollen analogues are circled. Thick lines represent five-point running averages. Modern temperature and precipitation values for Abisko are shown by vertical lines (dashed line represents calculated modern mean July air-temperature at Lake Tibetanus; Table 2). Sed. = fine-grained sedimentary carbonate (primarily *Chara* calcite); Pis. = *Pisidium* sp. mollusc aragonite; Can. = adult *Candona candida* ostracode calcite. The shaded zone in the isotope panel marks the initial period of limited influence of detrital carbonate contamination on the $\delta^{18}O_{Sed}$ record. The heavy dashed line represents the inferred record of $\delta^{18}O_P$ (oxygen-isotope composition of precipitation and ambient lakewater) after accounting for temperature effects on $\delta^{18}O_{Sed}$ as derived from the pollen-inferred mean July temperature record (lower ‰ scale; see equation 1). Average modern lakewater/groundwater $\delta^{18}O$ based on the data compiled in Table 3 (−14.5‰ V-SMOW), indicated by the dashed vertical line, correlates to a $\delta^{18}O_{Sed}$ value of −13.2‰ V-PDB based on surface-sediment data (filled circle; Table 6). July insolation data at 65°N obtained from Berger and Loutre (1991) are shown for comparison.

calibration data set and have pollen assemblages that today have a statistically significant relationship with climate. The reconstructions for five of the samples in the lower part of the record are less reliable as their pollen composition differs in some ways from the modern calibration data set. The reconstruction for the basal sample may be particularly open to question. Overall, the reconstruction diagnostic statistics suggest that, as many of the fossil pollen samples at Lake Tibetanus have good modern analogues and have good statistical fits to climate, the bulk of the Holocene pollen assemblages at the site and hence the past vegetation were probably in equilibrium with climate.

The quantitative pollen-inferred reconstructions (Figure 4) indicate mean annual precipitation of up to 600–800 mm (i.e., more than double values as compared to modern conditions) in the early Holocene and mean July temperatures 1.5–2°C higher than today between about 9000 and 5000 cal. BP. Modern temperature values were attained at about 2500 cal. BP. Diatom records from sites in the Abisko area (Bigler *et al.*, unpublished data) similarly indicate elevated mean July temperatures prior to 6000 cal. BP (*c*. 2°C higher than at present), followed by a successive temperature decline during the late Holocene. This climatic development, which agrees well with the conclusions drawn by Barnekow (2000) based on individual tree species, is corroborated by quantitative climate reconstructions from several other sites in the region. These include temperature and precipitation records based on pollen, chironomids and diatoms from Lake Vuoskojaurasj, 10 km east of Abisko (Bigler *et al.*, 2002), pollen-based temperature and precipitation records from Lake Tsuolbmajavri in northern Finland, *c*. 130 km to the northeast (Seppä and Birks, 2001), and temperature records based on diatoms, chironomids, pollen and near-infrared spectroscopy from Lake Sjuodjijaure in the Sarek Mountains, *c*. 150 km south of Lake Tibetanus (Rosén *et al.*, 2001).

Isotope hydrology

Composite monthly $\delta^{18}O$ values of precipitation collected at the Abisko Scientific Research Station (388 m a.s.l.) during the period 1975–91 are shown in Figure 5. The time-series reveals a clear, but subdued, seasonal cycle fluctuating about the long-term weighted annual average for 1975–90 of –13.4‰. Burgman *et al.* (1987) attributed the remarkably low average seasonal amplitude at Abisko (*c*. 2.5‰) compared to other sites in Sweden to the moderating influence of the nearby Atlantic Ocean.

Oxygen- and hydrogen-isotope data obtained on water samples from the lake and surrounding areas are presented in Table 3 and Figure 6. Though small, this data set yields important insights regarding the isotope hydrology of Lake Tibetanus. Lakewater $\delta^{18}O$ shows only minor fluctuations in the range of –15.0 to –13.5‰, which are evidently not related to seasonal changes in condensation temperature and $\delta^{18}O$ of precipitation in the area (Figure 5). The isotopic signatures of the lakewater also plot very close to corresponding values of recharging groundwater and to the tentative local meteoric waterline based on precipitation and groundwater data (Figure 6). Furthermore, groundwater and lakewater isotopic compositions exhibit intermediate values as compared to the broad range observed among individual precipitation samples from the Abisko area. These features indicate that lakewater $\delta^{18}O$ is controlled by $\delta^{18}O$ of local groundwater and that negligible evaporative enrichment of ^{18}O occurs during the short residence time in the lake. This, in turn, suggests that lakewater $\delta^{18}O$ should closely reflect the weighted mean annual $\delta^{18}O$ of precipitation falling within the lake's catchment. The slightly lower $\delta^{18}O$ values of groundwater at Lake Tibetanus as compared to the yearly average in precipitation at Abisko (Figure 5) are expected, given the higher elevation (cf. Siegenthaler and
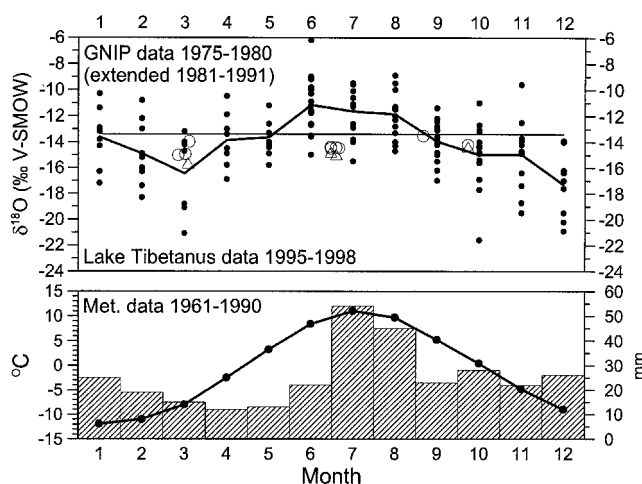
Figure 5 Composite monthly values of $\delta^{18}O$ in precipitation together with monthly mean values of precipitation and temperature for the period 1961–90 at the Abisko Scientific Research Station (6 km ENE of Lake Tibetanus at an altitude of 388 m a.s.l.; Figure 1). The isotopic data were collected during the period January 1975 to January 1991. Black dots refer to individual monthly samples (136 values in total) and the solid line represents monthly mean values. The long-term weighted annual mean for the years 1975–90 (straight line) is –13.4‰. $\delta^{18}O$ data obtained on lakewater (open circles) and recharging groundwater (triangles) at Lake Tibetanus (560 m a.s.l.) are shown for comparison (Table 3). Precipitation isotopic data for 1975–80 were derived from the GNIP (Global Network of Isotopes in Precipitation) data base maintained by IAEA and WMO, and supplemented by corresponding data for 1981–91 (Department of Earth Sciences, Uppsala University, unpublished data).
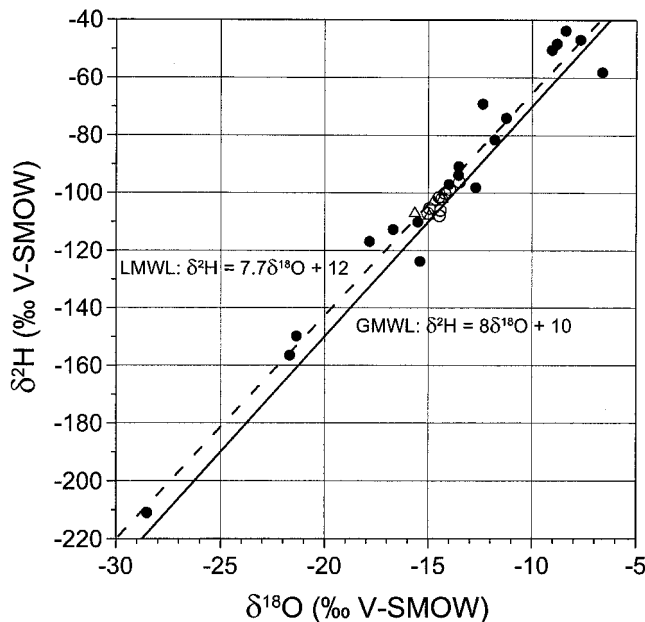
Figure 6 Plot of $\delta^{18}O$ versus δ^2H values for samples of snow and rain (filled circles) collected in the Abisko area, lakewater samples from Lake Tibetanus (open circles) and samples of groundwater recharging the lake (triangles; see Table 3 for details). GMWL is the global meteoric waterline (Craig, 1961) and LMWL is a tentative local meteoric waterline based on isotopic data obtained on samples of snow, rain and groundwater.

Oeschger, 1980) and resulting small difference in local mean annual temperature (Table 2). Notably, the combination of mean annual temperature (MAT; *c*. –1.4°C) estimated from meteorological data and the average $\delta^{18}O$ value of groundwater and lakewater samples (–14.5‰) falls almost exactly on the well-known 'Dansgaard line' ($\delta^{18}O_P = 0.7MAT – 13.6$; Dansgaard, 1964), which provides a useful reference for consideration of the spatial

and temporal isotope-temperature relations at Lake Tibetanus in the past (see further discussion below).

Given the physiographical setting of Lake Tibetanus and other evidence noted previously, similar open hydrologic conditions are likely to have prevailed throughout the lake's existence. As a result, endogenic carbonates formed in association with the lake-water and subsequently preserved in the sediments should carry a strong signal derived from the isotopic composition of local precipitation ($\delta^{18}O_P$).

Carbonate oxygen-isotope records

Origin of carbonates and intra-specific isotopic offsets

The oxygen-isotope records obtained from the Lake Tibetanus sequence are illustrated in Figure 3 and compiled in Table 6. These include 61 fine-grained sedimentary calcite samples ($\delta^{18}O_{Sed}$) spanning the full sequence, 48 samples of shells from *Pisidium* sp. ($\delta^{18}O_{Pis}$), and 26 samples of adult *Candona candida* valves ($\delta^{18}O_{Can}$). The last two records cover the upper 2.5 m. The three carbonates display remarkably consistent isotopic offsets, with *Pisidium* sp. and *C. candida* samples enriched in ^{18}O on average by 1.6 ± 0.3‰ and 2.9 ± 0.4‰, respectively, as compared to the co-existing sedimentary calcite. These systematic oxygen-isotope differences are also clearly apparent from the pronounced clustering of the data points for the three different carbonate components in a cross-plot incorporating the associated carbon-isotope data (Figure 2).

As for $\delta^{13}C$ (see Hammarlund *et al.*, 1997), the characteristic oxygen-isotope differences can be attributed to a combination of mineralogical, biological and temperature-dependent effects. For example, about 0.9‰ of the average $\delta^{18}O$ offset between the aragonite *Pisidium* shells and co-existing fine-grained sedimentary calcite derives from the combination of differing mineralogy (*c.* 0.6‰; Tarutani *et al.*, 1969) and 'vital offset' (*c.* 0.3‰; von Grafenstein *et al.*, 1999), yielding an average residual difference of *c.* 0.7‰ between these two components. This compares closely with the residual difference of *c.* 0.8‰ between the calcite *C. candida* valves and the sedimentary carbonate obtained after accounting for the vital offset of *c.* 2.1‰ documented for this ostracode species (von Grafenstein *et al.*, 1999). Evidence from recent studies of similar lake sediments from southern Sweden suggests that a small (<0.5‰) fixed kinetic isotope enrichment effect relative to theoretical 'equilibrium' calcite may also occur during precipitation of calcite on *Chara* algae via the proton pumping mechanism (Hammarlund *et al.*, 1997; 1999; McConnaughey, 1991), thus displacing the $\delta^{18}O_{Sed}$ record slightly closer towards $\delta^{18}O_{Pis}$ and $\delta^{18}O_{Can}$.

Taking these factors into consideration, it is clear that the average residual $\delta^{18}O$ difference between the fine-grained sedimentary calcite and both molluscs and ostracodes, corrected to a common equilibrium calcite, is probably of the order of *c.* 1‰. This offset can be ascribed mainly to differences in the average temperature of the lakewater at the respective times of carbonate formation, given that seasonal fluctuations in lakewater $\delta^{18}O$ should be strongly damped because of persistently rapid throughflow. Assuming a temperature sensitivity of *c.* –0.25‰/°C (Craig, 1965; Friedman and O'Neil, 1977) for carbonate-water equilibrium exchange under typical environmental conditions, this suggests that water temperatures during the main summer period of *Chara* photosynthesis in Lake Tibetanus (probably June–July) typically average about 4°C higher than during either the prolonged annual period of shell growth in *Pisidium* sp. or the short autumn period of calcification of adult *C. candida* valves (cf. von Grafenstein *et al.*, 1994). Integration of isotopic signals over a short seasonal 'window' with considerable year-to-year temperature variation by

Table 6 Carbon content and stable oxygen-isotope analysis results

Sample	Depth (m)	OC (%)	CC (%)	$\delta^{18}O_{Sed}$	$\delta^{18}O_{Pis}$	$\delta^{18}O_{Can}$
Surface	0.00	n.d	n.d	–13.22	n.d.	n.d.
1	0.00–0.06	18.4	2.89	–13.03	–11.45	–9.75
2	0.06–0.11	13.9	5.10	–12.97	–11.64	n.d.
3	0.11–0.15	14.2	5.36	–13.43	–11.95	–10.42
4	0.15–0.20	13.9	5.38	–13.16	–11.32	n.d.
5	0.20–0.25	13.7	5.17	–13.20	–10.99	–10.28
6	0.25–0.30	11.4	6.34	–13.38	–11.66	n.d.
7	0.30–0.34	14.1	5.81	–13.15	n.d.	–10.27
8	0.34–0.38	11.6	7.25	–13.24	–11.19	n.d.
9	0.38–0.45	10.8	8.36	–13.20	–11.74	–10.24
10	0.45–0.50	11.3	8.38	–13.06	–11.58	n.d.
11	0.50–0.56	12.1	7.56	–13.19	–11.57	–10.65
12	0.56–0.60	15.4	6.19	–13.30	–11.61	n.d.
13	0.60–0.65	15.8	5.64	–13.19	–11.25	–10.53
14	0.65–0.69	14.3	6.86	–12.89	–11.70	n.d.
15	0.69–0.74	11.7	7.79	–13.16	–11.59	–10.73
16	0.75–0.79	14.8	6.19	–13.35	–11.28	n.d.
17	0.79–0.84	8.24	9.32	–13.23	–11.70	–10.59
18	0.84–0.88	8.13	9.22	–12.85	–11.70	n.d.
19	0.88–0.92	18.9	3.72	–13.04	–11.50	–10.06
20	0.92–0.97	10.9	7.16	–13.05	–11.43	n.d.
21	0.97–1.03	7.40	8.98	–13.63	–11.42	–10.37
22	1.03–1.10	11.1	7.26	–13.27	–11.77	n.d.
23	1.10–1.16	15.8	4.85	–13.42	–11.68	–10.68
24	1.16–1.21	7.18	8.95	–13.48	n.d.	n.d.
25	1.21–1.27	10.7	7.88	–13.52	–11.79	–10.71
26	1.27–1.33	11.1	7.17	–13.44	n.d.	n.d.
27	1.33–1.39	8.30	8.56	–13.30	–12.04	–10.74
28	1.39–1.44	7.72	9.16	–13.29	–11.65	n.d.
29	1.44–1.48	9.22	8.90	–13.47	–11.90	–10.73
30	1.48–1.53	5.54	10.1	–13.69	–11.72	n.d.
31	1.53–1.58	7.84	9.28	–13.51	–11.77	–11.05
32	1.58–1.64	11.5	8.08	–13.26	–11.62	n.d.
33	1.64–1.68	9.29	8.68	–13.30	–11.68	–10.33
34	1.68–1.74	11.4	8.22	–13.42	–11.67	n.d.
35	1.74–1.78	16.8	5.64	–13.34	–11.39	–9.90
36	1.78–1.83	20.2	5.33	–13.53	–11.81	n.d.
37	1.83–1.88	8.01	9.37	–13.24	–11.91	–10.79
38	1.88–1.93	20.7	4.40	–12.90	–11.85	n.d.
39	1.93–1.97	12.3	8.26	–13.11	–11.91	–10.22
40	1.97–2.01	6.02	10.0	–13.73	–11.82	n.d.
41	2.01–2.07	2.25	10.8	–13.28	–11.85	–10.46
42	2.07–2.12	1.83	10.8	–13.92	–11.66	n.d.
43	2.12–2.16	2.01	10.9	–13.06	–11.73	–10.70
44	2.16–2.20	1.43	11.3	–12.72	–11.71	n.d.
45	2.20–2.25	1.43	11.4	–13.03	–11.71	–9.95
46	2.25–2.29	1.40	11.4	–12.96	–11.22	n.d.
47	2.29–2.34	1.94	11.2	–13.07	–11.35	–9.19
48	2.34–2.38	2.04	11.2	–13.10	–11.63	n.d.
49	2.38–2.42	1.88	11.3	–12.73	–11.40	–8.80
50	2.42–2.47	1.93	11.2	–12.69	–11.19	n.d.
51	2.47–2.52	1.95	11.2	–12.77	–11.24	–9.66
52	2.52–2.58	1.63	11.4	–12.46		
53	2.58–1.63	1.84	11.4	–12.36		
54	2.63–2.67	1.53	11.5	–12.17		
55	2.67–2.71	1.20	11.5	–11.95		
56	2.71–2.74	1.36	11.4	–11.56		
57	2.74–2.78	1.41	11.3	–11.40		
58	2.78–2.82	1.78	9.31	–11.29		
59	2.82–2.84	1.05	10.4	n.d.		
60	2.84–2.90	0.98	4.96	–11.03		
61	2.90–2.95	0.58	2.36	–10.99		

Isotopic units: ‰ (V-PDB). Sed. = fine-grained sedimentary carbonate (primarily *Chara* calcite). Pis. = *Pisidium* sp. mollusc aragonite. Can. = adult *Candona candida* ostracode calcite. n.d. = no determination.

C. candida is also suggested by the larger degree of scatter on Figure 2 as compared to the other two carbonate components.

As demonstrated by Hammarlund and Buchardt (1996), it is possible for isotopic records obtained on bulk carbonates from lacustrine deposits to be affected by detrital material originating from bedrock and soils in a lake's catchment, especially during cold episodes with unstable soils and shortly after deglaciation. However, based on several independent lines of evidence, this process never played an important role in the sediments of Lake Tibetanus. (1) As shown in Figure 2, the isotopic records obtained on fine-grained bulk carbonate follow an evolution towards the concentrated cluster of points from samples having $\delta^{13}C$ values well above those measured on calcite from the local marble. (2) *Chara* encrustations are very common in the lower part of the sequence except in the two lowermost samples. (3) A radiocarbon date obtained on bulk carbonates at 2.90–2.95 m (18030 ± 175 BP; Hammarlund *et al.*, 1997) gives evidence of a significant ^{14}C activity of carbonates already at the onset of sedimentation (*c.* 32% endogenic material). (4) Mineral magnetic data indicate a negligible erosional input after the initial 200–300 year period of the lake history (Berglund *et al.*, 1996). Furthermore, after *c.* 8000 cal. BP the close covariance with the corresponding mollusc and ostracode records gives additional evidence of an endogenic origin of the fine-grained calcite used for isotopic analysis.

Reconstruction of precipitation $\delta^{18}O$

The $\delta^{18}O_{Sed}$ profile provides the fullest stratigraphical record from Lake Tibetanus, extending from the earliest part of the lake's history to the present. Although the record may be offset to slightly higher $\delta^{18}O$ values than that of equivalent equilibrium calcite, as noted above, any stratigraphical fluctuations should be related primarily to changes in lakewater $\delta^{18}O$ inherited from variations in the isotopic composition of local precipitation ($\delta^{18}O_P$) plus secondary temperature-dependent variations in carbonate-water fractionation due to changes in summer lakewater temperature.

Compensation for a fixed non-equilibrium offset in the $\delta^{18}O_{Sed}$ record can be accomplished by relating the $\delta^{18}O_{Sed}$ value measured on surface sediments (–13.2‰ V-PDB) to the best estimate of modern local $\delta^{18}O_P$ (–14.5‰ V-SMOW), which is based on the average $\delta^{18}O$ of local groundwater and lakewater samples (see lower scale on Figure 4). Notably, in the absence of non-equilibrium effects, this comparison would yield a water temperature of +10.3°C (based on the equation $10^3\ln\alpha_{carbonate-water} = 2.78(10^6T^{-2}) - 2.89$ (Friedman and O'Neil, 1977), where T is water temperature in degrees Kelvin and $\alpha_{carbonate-water} = (1000 + \delta^{18}O_{carbonate})/(1000 + \delta^{18}O_{water})$, with $\delta^{18}O$ values expressed relative to a common standard, such that $\delta^{18}O_{V-PDB} = 1.03086$ $\delta^{18}O_{V-SMOW} + 30.86$ (Fritz and Fontes, 1980).) This is essentially identical to the estimated modern mean July temperature at Lake Tibetanus (*c.* +10.4°C; Table 2), which confirms that any non-equilibrium offset in the $\delta^{18}O_{Sed}$ values must be rather small.

The signal of changing lakewater temperature within the $\delta^{18}O_{Sed}$ record can also be constrained on the supposition that changes in summer lakewater temperature, integrated over the period of seasonal *Chara* algal productivity, probably closely approached changes in air temperature (cf. Livingstone *et al.*, 1999), as reconstructed from the pollen data. Thus, the component of the $\delta^{18}O_{Sed}$ record related exclusively to changes in lakewater $\delta^{18}O$, and ultimately to $\delta^{18}O_P$, can be approximated by adjusting each $\delta^{18}O_{Sed}$ value by the equilibrium fractionation coefficient of *c.* –0.25‰/°C multiplied by the change in mean July temperature (ΔT) inferred from the pollen record compared to the estimated present-day mean July temperature (+10.4°C);

$$\text{Inferred } \delta^{18}O_P = \delta^{18}O_{Sed} + (-0.25‰/°C * -\Delta T°C) \qquad (1)$$

As shown by the dashed line in Figure 4, derived from smoothed $\delta^{18}O_{Sed}$ and pollen-inferred mean July temperature records, the greatest effect occurred at the time of highest temperature *c.* 6000 cal. BP, amounting to *c.* +0.6‰, with diminished magnitude at times of lower pollen-inferred temperatures both prior to and following this event.

Discussion

The Holocene $\delta^{18}O_P$ history compared to independent vegetational data

In spite of the substantial loss of finer structure in the smoothing of the record, the inferred $\delta^{18}O_P$ history from Lake Tibetanus displays clear correspondence with the four major vegetational zones that succeeded the initial period of dwarf-shrub tundra in the catchment (Figure 4). Thus, maximum inferred $\delta^{18}O_P$ (–12.4‰) occurred in the earliest part of the subarctic birch woodland zone around 10000 cal. BP, with $\delta^{18}O_P$ values falling rapidly to *c.* –13.3‰ by the time subalpine birch woodlands had become established at *c.* 8800 cal. BP. Thereafter $\delta^{18}O_P$ values continued to decline progressively, though at a lower rate, to a minimum of *c.* –14.2‰ at the transition to boreal pine-birch forest at *c.* 6300 cal. BP. This zone is then marked by a brief but distinct rise in $\delta^{18}O_P$ to a maximum of *c.* –14.0‰ between 6000 and 5500 cal. BP, followed by a decline to the modern value (–14.5‰) by *c.* 4000 cal. BP. Modern $\delta^{18}O_P$ values persisted over the early and late parts of the subsequent subalpine birch woodland period, though with another modest oscillation to a maximum of *c.* –14.3‰ at *c.* 2000 cal. BP.

Even more striking correspondence is evident from comparison between the $\delta^{18}O_P$ record and the quantitative, pollen-inferred reconstructions of climate parameters. Key features in this regard include the similar overall trends in $\delta^{18}O_P$ and pollen-inferred mean annual precipitation, as well as examples of higher-frequency covariance, such as the similar fluctuations in both $\delta^{18}O_P$ and pollen-inferred mean annual precipitation throughout the late-Holocene subalpine birch woodland zone (especially 3500 cal. BP to present) and the fine-scale variability during the early part of the boreal pine-birch zone (*c.* 6300–5000 cal. BP). Some analogous similarities or correlations can also be drawn between inferred $\delta^{18}O_P$ and pollen-inferred mean July temperature, although the latter reconstruction to a minor extent has made an imprint on the inferred $\delta^{18}O_P$ record through the temperature calibration of $\delta^{18}O_{Sed}$ data. However, the most obvious feature of this comparison (as also between mean annual precipitation and pollen-inferred mean July temperature) is the strong difference in the main low-frequency trends, with the major fluctuations in $\delta^{18}O_P$ and pollen-inferred temperature being inverse over the early part of the record, prior to *c.* 6500 cal. BP. Since July temperatures are normally related positively to mean annual temperatures (e.g., see data from the Abisko area in Table 2), this shows the existence of 'non-Dansgaard' effects, which are contrary to the positive isotope-temperature relations that usually prevail at mid- and high latitudes (Dansgaard, 1964). Indeed, as illustrated in Figure 7, quantitative evaluation of variations in the temporal $\delta^{18}O_P$-MAT relation in the Abisko area is now possible, expressed here as deviations in per mil (‰) from the 'Dansgaard line', revealing remarkably strong, systematic shifts at submillennial timescales that clearly dominate the isotope-climate history and are undoubtedly linked to shifting atmospheric circulation in the region during the past 10000 years.

Hence, the combination of high pollen-inferred mean annual precipitation and a strong non-Dansgaard effect in the early Holocene corresponds with a rather warm and highly oceanic climate, as reflected by a vegetational composition dependent on moist soils (especially as indicated by high frequencies of pterido-phyte spores and *Salix* pollen), and certainly characterized by frequent cyclonic events and abundant precipitation (cf. Yu and Har-
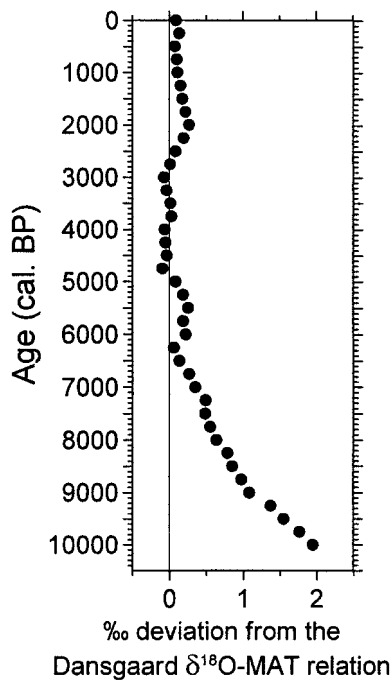
Figure 7 Evolution of the $\delta^{18}O_P$-MAT relation in the Abisko area expressed as 250-year average deviations ('non-Dansgaard' effects) from the relation: $\delta^{18}O_P = 0.7MAT - 13.6$ (Dansgaard, 1964). The $\delta^{18}O_P$ history is based on the $\delta^{18}O_{Sed}$ record from Lake Tibetanus, corrected for temperature-dependent equilibrium exchange between carbonate and lake-water, as shown in Figure 4. Inferred MAT (mean annual temperature) is calculated from pollen-inferred mean July temperature (MJT), also shown in Figure 4, based on the relation: $MAT = 0.23MJT - 3.8$ ($R^2 = 0.55$), derived from linear regression of local meteorological data (Table 2, Alexandersson *et al.*, 1991). The progressively diminishing magnitude of 'non-Dansgaard' effects during the early Holocene corresponds with progressively declining oceanicity. See text for further explanation.

rison, 1995). Notably, in spite of higher-than-present growing-season temperatures, boreal pine-birch forests were absent in the Abisko area for several millennia subsequent to deglaciation, probably due to high winter precipitation and late-melting snow. This pattern of vegetational change clearly differs from the development further south in the Scandes (Kullman, 1993; 1995), and possibly also compared to adjacent parts of northern Finland (Seppä and Weckström, 1999). The existence of substantial non-Dansgaard effects prior to *c.* 6500 cal. BP is consistent with efficient transfer of moisture across the Scandes Mountains and significant suppression of rain- and isotope-shadow effects at this time compared to the present (Dray *et al.*, 1998; cf. Edwards *et al.*, 1996).

Interestingly, subfossil wood from the shore of Lake Njulla (1000 m a.s.l.; Figure 1) dated to 8130–8540 ^{14}C years BP (*c.* 8700–9600 cal. BP; Kullman, 1999) suggests that scattered pines occurred at very high altitudes shortly after the deglaciation, though the co-existence of light-demanding plants such as *Dryas octopetala* and *Salix herbacea* in the sediments of Lake Njulla from this period argue for predominantly open vegetation, rather than forests of boreal character (Barnekow, 1999). This early-Holocene plant community, which is highly anomalous in comparison to modern plant communities in the region, may reflect the fundamentally different climate (i.e., both warmer and wetter, with greater summer insolation) that prevailed in the area as compared to present-day conditions (Figure 4). The altitudinal expansion of pine that did eventually occur in the Abisko valley *c.* 6000–4500 cal. BP (Barnekow, 2000), was probably a consequence of weakening oceanic influence and decreasing precipitation (Seppä and Hammarlund, 2000). This resulted in decreased penetration of westerlies, deepening the rain and isotope shadows

in the lee of the Scandes, and increased isotopic distillation of moisture (increased heavy-isotope depletion). Thus, the temporal $\delta^{18}O_P$-MAT relation (Dansgaard, 1964) characterizing present-day conditions in the area was established by about 6000 cal. BP.

The decrease in pollen-inferred mean July temperature that was initiated at *c.* 6000 cal. BP has apparently continued into the present (Figure 4), accompanied by modest, though possibly systematic, related deviations in both pollen-inferred mean annual precipitation and the temporal $\delta^{18}O_P$-MAT relation (Figure 7). This temperature decline, which was probably brought about by the continuing reduction in summer insolation, successively lowered the upper limit of boreal pine-birch forest in the area and led to the establishment of the subalpine belt of mountain birch that persists in the Scandes Mountains today (Kullman, 1992; Barnekow, 2000).

Causes and implications of temporal changes in $\delta^{18}O_P$-MAT relations

It is clear that a variety of mechanisms, in addition to increasing distillation, might have contributed to the strong apparent shift in the $\delta^{18}O_P$-MAT relation in the Abisko region during the early to mid-Holocene. These could include changes in the source area and isotopic composition of oceanic vapour, as well as the slight relative increase in the altitude of the Scandes Mountains resulting from isostatic rebound, although both of these effects are likely to have been fairly small. The $\delta^{18}O$ of North Atlantic surface water, for example, was probably approaching modern values by 10000–8000 cal. BP, since North Atlantic deep-water formation was fully re-established shortly after 10000 cal. BP (Lehman and Keigwin, 1992; Björck *et al.*, 1996), the bulk of the Northern Hemisphere ice sheets had already melted, and the total increase in $\delta^{18}O$ of the global ocean during the last glacial as compared to the present was only *c.* 0.8‰ anyway (Schrag *et al.*, 1996). Similarly, an increase in altitude of 40–70 m during the period of most rapid uplift (*c.* 9500 to 6500 cal. BP; Møller, 1987; N.-O. Svensson, personal communication) might have contributed a signal of up to 0.3‰, assuming typical lapse rates of *c.* –0.5‰/100 m (cf. Siegenthaler and Oeschger, 1980; Ingraham, 1998), if the altitude effect itself was not suppressed by the abundance of precipitation. Changes in the seasonal distribution of precipitation, i.e., progressively increasing relative contributions of isotopically depleted snow and rain being delivered to Lake Tibetanus during the early to mid-Holocene, could also be invoked, though it would be difficult to generate a reasonable mass balance, in light of the small modern annual range of $\delta^{18}O$ variation (Figure 5), which may have been even smaller at times of greater oceanicity as described below.

Thus, as suggested above, stronger zonal atmospheric circulation during the early Holocene remains the most plausible mechanism to explain the strong shifts in the $\delta^{18}O_P$-MAT relation. General circulation-model experiments (Huntley and Prentice, 1993), for example, indicate warm, moist summers and mild, moist winters in northern Scandinavia at 9000 cal. BP, consistent with our climate reconstructions. The high summer insolation at this stage apparently enhanced the sea-level air-pressure gradient between the North Atlantic and the Eurasian continent, which caused a deepening of the Icelandic Low and a stronger penetration of westerlies into the continent. This flow pattern, which resulted in high amounts of winter precipitation and mean winter temperatures more than 2°C higher than at present (Huntley and Prentice, 1993; Kutzbach *et al.*, 1993), may have been enhanced by ocean-circulation changes. Diatom records from the Greenland, Iceland and Norwegian Seas (Koç *et al.*, 1993) indicate extensive northward flow of warm Atlantic surface waters during the period of 10000–6000 cal. BP. This ocean-circulation pattern probably induced a steep east–west temperature and pressure gradient over the North Atlantic and thus a strong zonal atmospheric flow across

the northern part of the Scandes Mountains during the early Holocene. Recent isotopic and palaeoecological evidence also records this period of enhanced oceanic influence eastwards along the northern Eurasian coast, though without indications of any pronounced non-Dansgaard effects, presumably because of the absence of a significant upwind topographical barrier (Wolfe *et al.*, 2000).

Our results demonstrate the necessity and usefulness of considering possible changes with time in $\delta^{18}O_P$-MAT relations when interpreting oxygen-isotope records obtained from continental climate archives. This aspect of the complex isotope-climate coupling is often ignored, and several recently published studies have involved attempts to calibrate inferred $\delta^{18}O_P$ records or oxygen-isotope records dependent on $\delta^{18}O_P$ to air temperature based on assumptions of fixed $\delta^{18}O_P$-MAT relations over time. These include Holocene $\delta^{18}O$ records obtained on speleothem calcite from northern Norway (Lauritzen and Lundberg, 1999) *c.* 250 km southwest of Abisko, and lacustrine biogenic silica at a site less than 20 km east of Lake Tibetanus (Shemesh *et al.*, 2001). Both records exhibit depletion in ^{18}O with time during the course of the Holocene, although mainly confined to the period of 10000–8500 cal. BP at the Norwegian site (Lauritzen and Lundberg, 1999). The similar trends shared by these records and the present results, as well as by a Holocene $\delta^{18}O_P$ reconstruction based on lacustrine cellulose from mid-central Sweden (Hammarlund *et al.*, unpublished data), suggest that the major ocean-atmosphere climate dynamics discussed above influenced the $\delta^{18}O_P$ evolution at a regional scale, perhaps including even larger areas adjacent to the North Atlantic. Indeed, decoupling of $\delta^{18}O_P$ and temperature in this manner might also help to account for an early-Holocene decline in $\delta^{18}O$ of almost 3‰ recorded in lacustrine carbonates at a site in southwestern Ireland, otherwise leading to an estimated temperature decline of 6°C (Ahlberg *et al.*, 2001), seemingly excessive for this strongly oceanic setting.

Although further analysis and testing are obviously warranted, accumulating evidence is consistent with the hypothesis that 'non-Dansgaard' variations in $\delta^{18}O_P$-MAT relations in northwest Europe and northern North America (Edwards *et al.*, 1996) were linked to millennial-scale fluctuations in the strength of circumpolar zonal circulation. These fluctuations themselves would seem to be strongly analogous to increasingly well-documented decadal-scale modes of climate variability characterized variably as the North Atlantic Oscillation (NAO), the Arctic Oscillation (AO) or, more comprehensively, the Northern Hemisphere Annular Mode (NAM; Thompson and Wallace, 2001). Thus, significant potential may exist to test this hypothesis using atmospheric general circulation models equipped with water-isotope diagnostics (e.g., Jouzel *et al.,* 2000; Hoffmann *et al.*, 2000).

Conclusions

New constraints on palaeotemperature change provided by pollen-climate transfer functions strongly reinforce the notion that progressively changing $\delta^{18}O_P$-MAT relations with time characterized the isotope climate in the Abisko area from deglaciation around 10000 cal. BP to *c.* 6000 cal. BP. We attribute these early-Holocene 'non-Dansgaard' effects to reduced distillation of moisture traversing the Scandes Mountains under the influence of intense westerly circulation, which gradually subsided in response to declining atmospheric zonal index. At a local scale, this phenomenon can be viewed as the result of a deepening isotopic shadow effect, analogous to those observed on the lee side of some mountain ranges (Siegenthaler and Oeschger, 1980; Dray *et al.*, 1998), essentially reflecting a response to changes in the efficiency of moisture transport across a topographical barrier. Smaller fluctuations in the atmospheric zonal index may be responsible for sub-

sequent minor variations in the apparent temporal $\delta^{18}O_P$-MAT relation at the submillennial scale localized around the expected Dansgaard relation over the past 6000 years, and such variability is likely to be a key feature of future isotope climate in the Abisko region. It is important to note that these 'non-Dansgaard' effects, which constitute fundamental isotope-climate signals, can only be derived by coupling independent palaeorecords, thus strongly supporting the use of a multiproxy approach to reconstruct or constrain past climate.

Acknowledgements

References

Ahlberg, K., Almgren, E., Wright, H.E. Jr and **Ito, E.** 2001: Holocene stable-isotope stratigraphy at Lough Gur, County Limerick, western Ireland. *The Holocene* 11, 367–72.
Alexandersson, H., Karlström, C. and **Larsson-McCann, S.** 1991: Temperature and precipitation in Sweden, 1961–90. Reference normals. Swedish Meteorological and Hydrological Institute, Meteorologi 81. Norrköping, Sweden.
Amundson, R., Chadwick, O., Kendall, C., Wang, Y. and **DeNiro, M.** 1996: Isotopic evidence for shifts in atmospheric circulation patterns during the late Quaternary in mid-North America. *Geology* 24, 23–26.
Barnekow, L. 1999: Holocene tree-line dynamics and inferred climatic changes in the Abisko area, northern Sweden, based on macrofossil and pollen records. *The Holocene* 9, 253–65.
—— 2000: Holocene regional and local vegetation history and lake-level changes in the Torneträsk area, northern Sweden. *Journal of Paleolimnology* 23, 399–420.
Barnekow, L., Possnert, G. and **Sandgren, P.** 1998: AMS ^{14}C chronologies of Holocene lake sediments in the Abisko area, northern Sweden – a comparison between dated bulk sediment and macrofossil samples. *GFF* 120, 59–67.
Berger, A. and **Loutre, M.F.** 1991: Insolation values for the climate of the last 10 million years. *Quaternary Science Reviews* 10, 297–317.
Berglund, B.E., Barnekow, L., Hammarlund, D., Sandgren, P. and **Snowball, I.F.** 1996: Holocene forest dynamics and climate changes in the Abisko area, northern Sweden – the Sonesson model of vegetation history reconsidered and confirmed. *Ecological Bulletins* 45, 15–30.
Bigler, C., Larocque, I., Peglar, S.M., Birks, H.J.B. and **Hall, R.I.** 2002: A quantitative multiproxy study of Holocene environmental change from a small lake near Abisko, northern Sweden. *The Holocene*, in press.

Birks, H.J.B. 1995: Quantitative palaeoenvironmental reconstructions. In Maddy, D. and Brew, J.S., editors, *Statistical modelling of Quaternary science data*, Cambridge: Cambridge Quaternary Research Association, 161–254.

—— 1998: Numerical tools in palaeolimnology – progress, potentialities, and problems. *Journal of Paleolimnology* 20, 307–32.

Birks, H.J.B., Line, J.M., Juggins, S., Stevenson, A.C. and **ter Braak, C.J.F.** 1990: Diatoms and pH reconstruction. *Philosophical Transactions of the Royal Society of London* B327, 263–78.

Björck, S., Kromer, B., Johnsen, S., Bennike, O., Hammarlund, D., Lemdahl, G., Possnert, G., Rasmussen, T.L., Wohlfarth, B., Hammer, C.U. and **Spurk, M.** 1996: Synchronized terrestrial-atmospheric deglacial records around the North Atlantic. *Science* 274, 1155–60.

Buchardt, B. 1977: Oxygen isotope ratios from shell material from the Danish Middle Paleocene (Selandian) deposits and their interpretation as paleotemperature indicators. *Palaeogeography, Palaeoclimatology, Palaeoecology* 22, 209–30.

Burgman, J.O., Calles, B. and **Westman, F.** 1987: Conclusions from a ten year study of oxygen-18 in precipitation and runoff in Sweden. Symposium on Isotope Techniques in Water Resources Development, International Atomic Energy Agency, Vienna, 30 March – 3 April, IAEA-SM-299/107, 579–90.

Charles, C.D., Rind, D., Jouzel, J., Koster, R.D. and **Fairbanks, R.G.** 1994: Glacial-interglacial changes in moisture sources for Greenland: influence on the ice core record of climate. *Science* 263, 508–11.

Coleman, M.L., Shepherd, T.J., Durham, J.J., Rouse, J.E. and **Moore, G.R.** 1982: Reduction of water with zinc for hydrogen isotope analysis. *Analytical Chemistry* 54, 993–95.

Coplen, T.B. 1996: New guidelines for reporting stable hydrogen, carbon, and oxygen isotope-ratio data. *Geochimica et Cosmochimica Acta* 60, 3359–60.

Craig, H. 1961: Standards for reporting concentrations of deuterium and ^{18}O in natural waters. *Science* 133, 1833–34.

—— 1965: The measurement of oxygen isotope palaeotemperatures. In Tongiorgi, E., editor, *Stable isotopes in oceanographic studies and palaeotemperatures*, Pisa: Consiglio Nazionale delle Ricerche, 161–82.

Dahl, S.O. and **Nesje, A.** 1996: A new approach to calculating Holocene winter precipitation by combining glacier equilibrium-line altitudes and pine-tree limits: a case study from Hardangerjøkulen, Norway. *The Holocene* 6, 381–98.

Dansgaard, W. 1964: Stable isotopes in precipitation. *Tellus* 16, 436–68.

Dray, M., Jusserand, C., Novel, J.P. and **Zuppi, G.M.** 1998: Air mass circulation and the isotopic 'shadow effect' in precipitation in the French and Italian Alps. Symposium on Isotope Techniques in the Study of Past and Current Environmental Changes in the Hydrosphere and in the Atmosphere, International Atomic Energy Agency, Vienna, 14–18 April, IAEA-SM-349/10, 107–17.

Edwards, T.W.D., Wolfe, B.B. and **MacDonald, G.M.** 1996: Influence of changing atmospheric circulation on precipitation δ^{18}O-temperature relations in Canada during the Holocene. *Quaternary Research* 46, 211–18.

Ekman, S. 1957: Die Gewässer des Abisko-Gebietes und Ihre Bedingungen. *Proceedings of the Royal Swedish Academy of Sciences* 4th series, volume 6, no. 6.

Epstein, S. and **Mayeda, T.** 1953: Variation of ^{18}O content of waters from natural sources. *Geochimica et Cosmochimica Acta* 4, 213–24.

Friedman, I. and **O'Neil, J.R.** 1977: Compilation of stable isotope fractionation factors of geochemical interest. In *Data of Geochemistry* (sixth edition), Chapter KK, Washington, DC: United States Geological Survey, Professional Paper 440-KK.

Fritz, P. and **Fontes, J.-Ch.** 1980: Introduction. In Fritz, P. and Fontes, J.-Ch., editors, *Handbook of environmental isotope geochemistry, volume 1, the terrestrial environment, A*, New York: Elsevier, 1–19.

Hammarlund, D. and **Buchardt, B.** 1996: Composite stable isotope records from a Late Weichselian lacustrine sequence at Grænge, Lolland, Denmark: evidence of Allerød and Younger Dryas environments. *Boreas* 26, 8–22.

Hammarlund, D. and **Edwards, T.W.D.** 1998: Evidence of changes in moisture transport efficiency across the Scandes Mountains in northern Sweden during the Holocene, inferred from lacustrine oxygen isotope records. Symposium on Isotope Techniques in the Study of Past and Current Environmental Changes in the Hydrosphere and in the Atmosphere. Inter-

national Atomic Energy Agency, Vienna, 14–18 April, IAEA-SM-349/40, 573–80.

Hammarlund, D. and **Lemdahl, G.** 1994: A late Weichselian stable isotope stratigraphy compared with biostratigraphical data: a case study from southern Sweden. *Journal of Quaternary Science* 9, 13–31.

Hammarlund, D., Aravena, R., Barnekow, L., Buchardt, B. and **Possnert, G.** 1997: Multi-component carbon isotope evidence of early Holocene environmental change and carbon-flow pathways from a hardwater lake in northern Sweden. *Journal of Paleolimnology* 18, 219–33.

Hammarlund, D., Edwards, T.W.D., Björck, S., Buchardt, B. and **Wohlfarth, B.** 1999: Climate and environment during the Younger Dryas (GS-1) as reflected by composite stable isotope records of lacustrine carbonates at Torreberga, southern Sweden. *Journal of Quaternary Science* 14, 17–28.

Hoffmann, G., Jouzel, J. and **Masson, V.** 2000: Stable water isotopes in atmospheric general circulation models. *Hydrological Processes* 14, 1385–406.

Huntley, B. and **Prentice, I.C.** 1993: Holocene vegetation and climates of Europe. In Wright, H.E. Jr., Kutzbach, J.E., Webb, T. III, Ruddiman, W.F., Street-Perrott, F.A. and Bartlein, P.J., editors, *Global climates since the last glacial maximum*, Minneapolis: University of Minnesota Press, 136–68.

Ingraham, N.L. 1998: Isotopic variations in precipitation. In Kendall, C. and McDonnell, J.J., editors, *Isotope tracers in catchment hydrology*, Amsterdam: Elsevier, 87–118.

Jonasson, C. 1991: Holocene slope processes of periglacial mountain areas in Scandinavia and Poland. PhD thesis, Uppsala University, Department of Physical Geography, report no. 79.

Josefsson, M. 1990: The geoecology of subalpine heaths in the Abisko valley, northern Sweden. PhD thesis, Uppsala University, Department of Physical Geography, report no. 78.

Joussaume, S. and **Jouzel, J.** 1993: Paleoclimatic tracers: an investigation using an atmospheric general circulation model under ice age conditions. 2. Water isotopes. *Journal of Geophysical Research* 98, 2807–30.

Jouzel, J., Hoffmann, G., Koster, R.D. and **Masson, V.** 2000. Water isotopes in precipitation: Data/model comparison for present-day and past climates. *Quaternary Science Reviews* 19, 363–79.

Jouzel, J., Koster, R. and **Joussaume, S.** 1996: Climate reconstruction from water isotopes: what do we learn from climate models? In Bradley, R.S., Jouzel, J. and Jones, P.D., editors, *Climate variations and forcing mechanisms of the last 2000 years,* Berlin: Springer-Verlag, 213–41.

Karlén, W. and **Kuylenstierna, J.** 1996: On solar forcing of Holocene climate: evidence from Scandinavia. *The Holocene* 6, 359–65.

Koç, N., Janssen, E. and **Haflidason, H.** 1993: Paleoceanographic reconstructions of surface ocean conditions in the Greenland, Icelandic and Norwegian Seas through the last 14 ka based on diatoms. *Quaternary Science Reviews* 12, 115–40.

Kulling, O. 1964: Bedrock map of the western part of the Torneträsk area. *Geological Survey of Sweden* Ser. Ba, No. 19.

Kullman, L. 1988: Holocene history of the forest-alpine tundra ecotone in the Scandes Mountains (central Sweden). *New Phytologist* 108, 101–10.

—— 1992: Orbital forcing and tree-limit history: hypothesis and preliminary interpretation of evidence from Swedish Lapland. *The Holocene*, 2, 131–37.

—— 1993: Holocene thermal trend inferred from tree-limit history in the Scandes Mountains. *Global Ecology and Biogeography Letters* 2, 181–88.

—— 1995: Holocene tree-limit and climate history from the Scandes Mountains Sweden. *Ecology* 76, 2490–502.

—— 1999: Early Holocene tree growth at a high elevation site in the northernmost Scandes of Sweden (Lapland): a palaeobiogeographical case study based on megafossil evidence. *Geografiska Annaler* 81A, 63–74.

Kutzbach, J.E., Guetter, P.J., Behling, P.J. and **Selin, R.** 1993: Simulated climatic changes: results of the COHMAP climate-model experiments. In Wright, H.E. Jr, Kutzbach, J.E., Webb, T. III, Ruddiman, W.F., Street-Perrott, F.A. and Bartlein, P.J., editors, *Global climates since the last glacial maximum*, Minneapolis: University of Minnesota Press, 24–93.

Laaksonen, K. 1976: The dependence of mean air temperatures upon latitude and altitude in Fennoscandia (1921–1950). *Annales Academiae Scientiarum Fennicae* 119, series A, 5–19.

Lauritzen, S.-E. and **Lundberg, J.** 1999: Calibration of the speleothem delta function: an absolute temperature record for the Holocene in northern Norway. *The Holocene* 9, 659–69.

Lehman, S.J. and **Keigwin, L.D.** 1992: Sudden changes in North Atlantic circulation during the last deglaciation. *Nature* 356, 757–62.

Livingstone, D.M., Lotter, A.F. and **Walker, I.R.** 1999: The decrease in summer surface water temperature with altitude in Swiss alpine lakes: a comparison with air temperature lapse rates. *Arctic, Antarctic, and Alpine Research* 31, 341–52.

MacDonald, G.M., Edwards, T.W.D., Moser, K.A., Pienitz, R. and **Smol, J.P.** 1993: Rapid response of treeline vegetation and lakes to past climate warming. *Nature* 361, 243–46.

Matthews, J.A., Dahl, S.O., Nesje, A., Berrisford, M.S. and **Andersson, C.** 2000: Holocene glacier variations in central Jotunheimen, southern Norway based on distal glaciolacustrine sediment cores. *Quaternary Science Reviews* 19, 1625–47.

McConnaughey, T.A. 1991: Calcification in *Chara corallina*: CO_2 hydroxylation generates protons for bicarbonate assimilation, *Limnology and Oceanography* 36, 619–28.

McCrea, J.M. 1950: On the isotopic chemistry of carbonates and a paleotemperature scale. *Journal of Chemical Physics* 18, 849–57.

McKenzie, J.A. and **Hollander, D.J.** 1993: Oxygen-isotope record in recent carbonate sediments from Lake Greifen, Switzerland (1750–1986): Application of continental isotopic indicator for evaluation of changes in climate and atmospheric circulation patterns. In Swart, P., Lohmann, K.C., McKenzie, J.A. and Savin, S., editors, *Climate change in continental isotopic records*, American Geophysical Union, Geophysical Monograph 78, 101–11.

Møller, J.J. 1987: Shoreline relation and prehistoric settlement in northern Norway. *Norsk Geografisk Tidsskrift* 41, 45–60.

Ovhed, M. and **Holmgren, B.** 1996: Modelling and measuring evapotranspiration in a mountain birch forest. *Ecological Bulletins* 45, 31–44.

Plummer, L.N. 1993: Stable isotope enrichment in paleowaters of the Southeast Atlantic Coastal Plain, United States. *Science* 262, 2016–20.

Renberg, I. 1991: The HON-Kajak sediment corer. *Journal of Paleolimnology* 6, 167–70.

Rosén, P., Segerström, U., Eriksson, L., Renberg, I. and **Birks, H.J.B.** 2001: Holocene climatic change reconstructed from diatoms, chironomids, pollen and near-infrared spectroscopy at an alpine lake (Sjuodjijaure) in northern Sweden. *The Holocene* 11, 551–62.

Schrag, D.P., Hampt, G. and **Murray, D.W.** 1996: Pore fluid constraints on the temperature and oxygen isotopic composition of the glacial ocean. *Science* 272, 1930–32.

Schwalb, A., Locke, S.M. and **Dean, W.E.** 1995: Ostracode $\delta^{18}O$ and $\delta^{13}C$ evidence of Holocene environmental changes in the sediments of two Minnesota lakes. *Journal of Paleolimnology* 14, 281–96.

Seppä, H. and **Birks, H.J.B.** 2001: July mean temperature and annual precipitation trends during the Holocene in the Fennoscandian tree-line area: pollen-based climate reconstructions. *The Holocene* 11, 527–39.

Seppä, H. and **Hammarlund, D.** 2000: Pollen-stratigraphical evidence of Holocene hydrological change in northern Fennoscandia supported by independent isotopic data. *Journal of Paleolimnology* 24, 69–79.

Seppä, H. and **Weckström, J.** 1999: Holocene vegetational and limnological changes in the Fennoscandian tree-line area as documented by pollen and diatom records from Lake Tsuolbmajavri, Finland. *Ecoscience* 6, 621–35.

Shemesh, A., Rosqvist, G., Rietti-Shati, M., Rubensdotter, L., Bigler, C., Yam, R. and **Karlén, W.** 2001: Holocene climatic change in Swedish Lapland inferred from an oxygen-isotope record of lacustrine biogenic silica. *The Holocene* 11, 447–54.

Siegenthaler, U. and **Oeschger, H.** 1980: Correlation of ^{18}O in precipitation with temperature and altitude. *Nature* 285, 314–17.

Sjörs, H. 1963: Amphi-Atlantic zonation, Nemoral to Arctic. In Löve, A. and Löve, D., editors, *North Atlantic biota and their history*, Oxford: Pergamon Press, 109–25.

Snowball, I.F. 1995: Mineral magnetic and geochemical properties of Holocene sediments and soils in the Abisko region of northern Sweden. *Department of Quaternary Geology, Lund University, Thesis* 34, 1–26.

Sonesson, M. 1974: Late Quaternary development of the Torneträsk area, North Sweden: 2. Pollen analytical evidence. *Oikos* 25, 288–307.

Stuiver, M., Reimer, P.J., Bard, E., Beck, J.W., Burr, G.S., Hughen, K.A., Kromer, B., McCormac, G., van der Plicht, J. and **Spurk, M.** 1998: NTCAL98 radiocarbon age calibration, 24000–0 cal BP. *Radiocarbon* 40, 1041–83.

Stute, M. and **Talma, A.S.** 1998: Glacial temperatures and moisture transport regimes reconstructed from noble gases and $\delta^{18}O$, Stampriet aquifer, Namibia. Symposium on Isotope Techniques in the Study of Past and Current Environmental Changes in the Hydrosphere and in the Atmosphere, International Atomic Energy Agency, Vienna, 14–18 April, IAEA-SM-349/53, 307–18.

Tarutani, T., Clayton, R.N. and **Mayeda, T.K.** 1969: The effect of polymorphism and magnesium substitution on oxygen isotope fractionation between calcium carbonate and water. *Geochimica et Cosmochimica Acta* 33, 987–96.

ter Braak, C.J.F. 1995: Non-linear methods for multivariate statistical calibration and their use in palaeoecology: a comparison of inverse (*k*-nearest neighbours, partial least squares, and weighted averaging partial least squares) and classical approaches. *Chemometrics and Intelligent Laboratory Systems* 28, 165–80.

ter Braak, C.J.F. and **Juggins, S.** 1993: Weighted averaging partial least squares regression (WA-PLS): an improved method for reconstructing environmental variables from species assemblages. *Hydrobiologia* 269/270, 485–502.

ter Braak, C.J.F. and **Šmilauer, P.** 1998: *CANOCO for Windows: software for canonical community ordination (version 4).* Ithaca, NY: Microcomputer Power, 351 pp.

ter Braak, C.J.F., Juggins, S., Birks, H.J.B. and **van der Voet, H.** 1993: Weighted averaging partial least squares regression (WA-PLS): definition and comparison with other methods for species–environment calibration. In Patil, G.P. and Rao, C.R., editors, *Multivariate environmental statistics*, Amsterdam: Elsevier, 525–60.

Thompson, D.W.J. and **Wallace, J.M.** 2001: Regional climate impacts of the Northern Hemisphere annular mode. *Science* 293, 85–89.

von Grafenstein, U., Erlenkeuser, H., Kleinmann, A., Müller, J. and **Trimborn, P.** 1994: High-frequency climatic oscillations during the last deglaciation as revealed by oxygen-isotope records of benthic organisms (Ammersee, southern Germany). *Journal of Paleolimnology* 11, 349–57.

von Grafenstein, U., Erlenkeuser, H. and **Trimborn, P.** 1999: Oxygen and carbon isotopes in modern fresh-water ostracod valves: assessing vital offsets and autecological effects of interest for palaeoclimate studies. *Palaeogeography, Palaeoclimatology, Palaeoecology* 148, 133–52.

Wolfe, B.B., Edwards, T.W.D., Aravena, R., Forman, S.L., Warner, B.G., Velichko, A.A. and **MacDonald, G.M.** 2000: Holocene paleohydrology and paleoclimate at treeline, north-central Russia, inferred from oxygen isotope records in lake sediment cellulose. *Quaternary Research* 53, 319–29.

Yu, G. and **Harrison, S.P.** 1995: Holocene changes in atmospheric circulation patterns as shown by lake status changes in northern Europe. *Boreas* 24, 260–68.